

# Sensor Information Analysis for a Humanoid Robot

Sooyong Lee\* and Paul Y. Oh

**Abstract:** For a humanoid robot to safely walk in unknown environments, various sensors are used to identify the surface condition and recognize any obstacles. The humanoid robot is not fixed on the surface and the base/orientation of the kinematics change while it is walking. Therefore, if the foot contact changes from the estimated due to the unknown surface condition, the kinematics results are not correct. The robot may not be able to perform the motion commands based on the incorrect surface condition. Some robots have built-in range sensors but it's difficult to accurately model the surface from the sensor readings because the movement of the robot should be considered and the robot localization should have zero error for correct interpretation of the sensor readings. In this paper, three infrared range sensors are used in order to perceive the floor state. Covariance analysis is incorporated to consider the uncertainties. The accelerometer and gyro sensor are also used in order to detect the moment a foot hits the surface. This information provides correction to the motion planner and robot kinematics when the environment is not modeled correctly.

**Keywords:** Contact state estimation, deadreckoning, floor state estimation.

## 1. INTRODUCTION

A humanoid robot has high mobility because it walks while avoiding obstacles. A lot of work has been done in humanoid robot running [1], walking on uneven surfaces or slopes [2]. Going up/down stairs [3] is another important function of the humanoid robot. However, such works have been implemented in a priori known environments. Unless complete floor information is available, dead reckoning becomes much less reliable because the robot kinematics is an open chain for most of the time except when two legs touch the floor at the same time, and the base of the kinematics may not be as expected if the floor condition is not known. In such cases, the humanoid robot may not be even able to walk safely. Unless extrinsic localization is used, the interaction between the robot and the floor should be monitored for localization and also for safety.

In unknown environments, the robot should sense obstacles and safely avoid them by modifying its path accordingly. Sensing obstacles is one of the major functions of a humanoid robot. Vision is commonly used for identifying obstacles and estimating their distance. A

stereo camera provides depth information as well as obstacle identification. However, the vision system's performance depends on illumination, color and material properties of the obstacle. It is hard to estimate multiple objects concurrently [4], and it may require heavy computing power [5]. Depth information resolution is not as high as other range sensors [6].

A humanoid robot does not have a fixed base and it is also important to estimate its attitude to perform tasks. In [7], 3D attitude sensors (inclinometer and accelerometer, gyro) are used to mimic the human vestibular system.. These sensors have drift errors and multiple sensors are used in order to remove them [8]. Use of a Kalman filter [9,10] is a common approach for addressing such errors..

Two types of sensors are used in this research; one for floor state estimation and another for floor contact recognition. Optical range sensors such as infrared ones and laser range finders, provide accurate measurements but they may not be able to detect glass. In addition, laser sensors are expensive and should be handled with caution due to safety. Furthermore, optical sensors are not robust to changing environmental light conditions. Ultrasonic sensors may not be as accurate as infrared ones however, they have longer measurement range; their beam angles are much wider than those of optical sensors. As such, it is difficult to differentiate object shape due to their wide beam angles. It's also difficult to tell whether the surface is flat or not, which may be very critical information to a humanoid robot. In this paper, three infrared range sensors are used in order to sense surfaces. Our main concern is unexpected non-flat surfaces. By taking advantage of the infrared range sensors' narrow beam, three sensors are installed radially and each sensor provides its measurement without interfering with each other. By analyzing the three range sensor values, the state of the floor can be successfully

Manuscript received November 22, 2013; revised March 7, 2014; accepted May 9, 2014. Recommended by Associate Editor Euntai Kim under the direction of Editor Hyouk Ryeol Choi.

This work was supported by the National Research Foundation of Korea Grant funded by the Korean Government MEST, Basic Research Promotion Fund (NRF-2010-013-D00005)

Sooyong Lee is with the Department of Mechanical and System Design Engineering, Hongik University, Seoul, Korea (e-mail: sooyong@hongik.ac.kr).

Paul Y. Oh is with the Department of Mechanical Engineering and Mechanics, Drexel University, Philadelphia, PA, USA (e-mail: paul@coe.drexel.edu).

\* Corresponding author.

differentiated. In [11], a similar sensor system is used for blind people to detect stairs.

An accelerometer and gyros are used to detect floor contact so that the robot motion planner, kinematics, and dead-reckoning are updated. The information from these sensors is very effective when an environment model is inaccurate or unavailable.

In the following sections, the kinematic models of the robot and the sensor system are described, the analysis of the sensor information with the experimental results is presented, and finishes with the conclusion.

## 2. HUMANOID ROBOT

The humanoid robot used in this paper is driven by Dynamixel AX-12 motors from Robotis, Inc. Each motor is controlled with a resolution of 300/1024 degree. Its maximum torque is 10 kgf·cm at 20 rpm. The robot is small and light-weight with high torque actuators. Therefore, we assume that each joint's position error is negligible at high bandwidths. With each joint's angle measurement, the position and orientation relative to the initial configuration can be estimated from the forward kinematics of the robot. Each leg has six degrees of freedom. The upper body and head movements are not considered because all the sensors are installed at the waist.

The robot's absolute position and orientation information is not available because no extrinsic localization system is used. For instance, if the robot is walking on unknown non-flat surfaces and if dead reckoning is the only available method for localization, the localization error accumulates as the robot moves. It is very important to perceive the condition of the surface the robot is walking on. The foot of the robot is a rigid link and the zero moment point varies from the heel, sole and toe. Therefore, the contact between the foot and

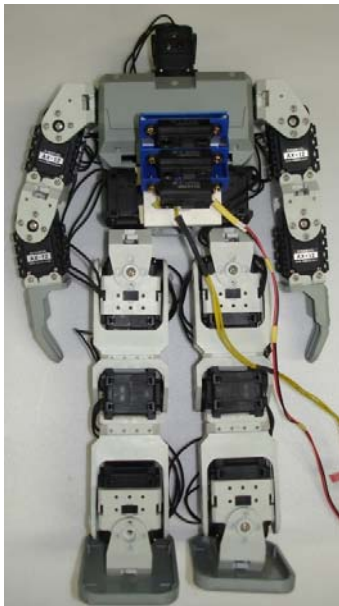


Fig. 1. Humanoid robot with infrared range sensor system.

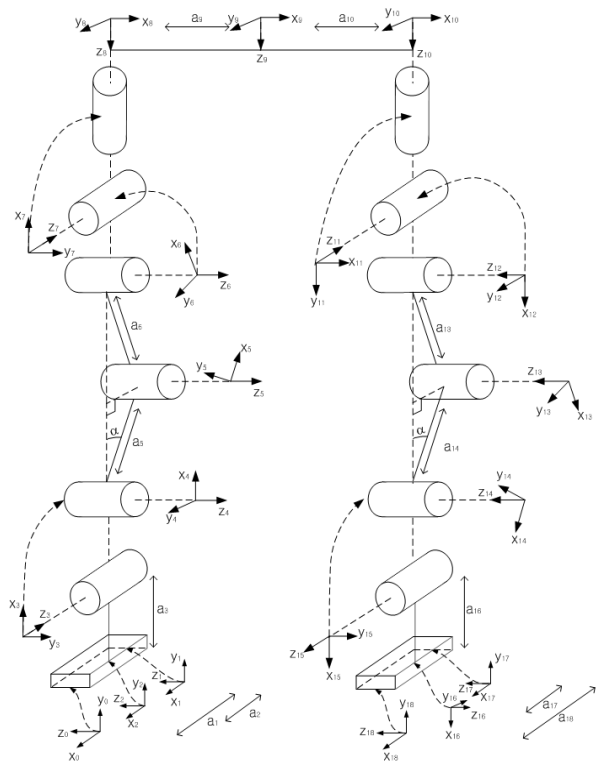


Fig. 2. Joint diagram.

surface sets the base orientation and the offset for the open forward kinematics.

Robot kinematics equations are not described in this paper due to their length. Instead, the joint diagram of the robot's two legs and waist is shown in the following figure.

## 3. SENSOR INFORMATION ANALYSIS

Sharp GP2Y0A710K infrared range sensors are used in this work.. These sensors can measure ranges from 80-to-500 cm and their resolution degrades range increases. The sensor system is composed of three infrared range sensors which are installed radially as shown in Fig. 3. The three sensors operate concurrently. The beam width of each infrared range sensor is narrow enough that they do not interfere with each other. Fig. 4 shows the sensor system configuration. The lower infrared sensor (S1) is orientated at an angle  $\alpha$  with respect to the gravity



Fig. 3. Infrared range sensor system.

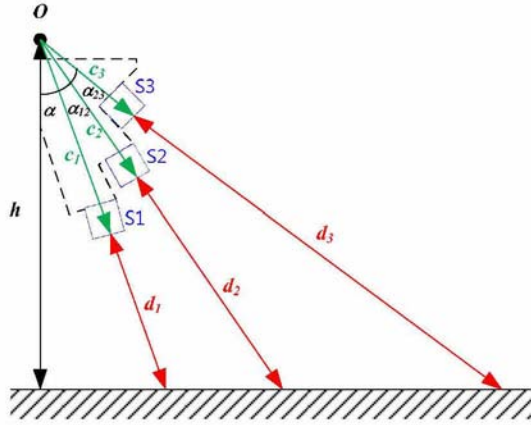


Fig. 4. Simplified sensor system model.

Table 1. Parameters.

parameter	representation	Value
$H$	distance from the floor to the origin of the sensor system	260 mm
$\alpha$	angle of the 1 <sup>st</sup> sensor ray from the gravity direction	20°
$\alpha_{12}$	angle between the 1 <sup>st</sup> sensor ray and the 2 <sup>nd</sup> sensor ray	15°
$\alpha_{23}$	angle between the 2 <sup>nd</sup> sensor ray and the 3 <sup>rd</sup> sensor ray	15°
$c_1$	distance from the sensor origin to tip of the 1 <sup>st</sup> sensor	71 mm
$c_2$	distance from the sensor origin to tip of the 2 <sup>nd</sup> sensor	60 mm
$c_3$	distance from the sensor origin to tip of the 3 <sup>rd</sup> sensor	49 mm
$d_1$	1 <sup>st</sup> sensor reading	
$d_2$	2 <sup>nd</sup> sensor reading	
$d_3$	3 <sup>rd</sup> sensor reading	

direction when the robot is at its home position. The center (S2) and upper (S3) sensors are installed  $\alpha_{12}$  and  $\alpha_{23}$  apart radially and at the distance of  $c_2$ ,  $c_3$  from the sensor system origin, respectively. The sensor system's origin is at height  $h$  at home position. Each sensor provides the range information,  $d_1$ ,  $d_2$  and  $d_3$  from the tip of the sensor to the floor surface (or to the obstacle).

The sensor system model is developed for perception of the floor state from the sensor information. Based on sensor reading changes, the change in floor state can be determined. Therefore, the sensor system is modeled in terms of sensor value changes instead of current values. The parameter values are shown in Table 1.

Let

$$L_1 = c_1 + d_1, \quad (1)$$

$$L_2 = c_2 + d_2, \quad (2)$$

$$L_3 = c_3 + d_3, \quad (3)$$

then, from the model one has

$$h = L_1 \cos \alpha, \quad (4)$$

$$h = L_2 \cos(\alpha + \alpha_{12}), \quad (5)$$

$$h = L_3 \cos(\alpha + \alpha_{12} + \alpha_{23}). \quad (6)$$

Because  $c_1$ ,  $c_2$ ,  $c_3$  are constants,

$$\Delta L_1 = \Delta d_1, \quad (7)$$

$$\Delta L_2 = \Delta d_2, \quad (8)$$

$$\Delta L_3 = \Delta d_3. \quad (9)$$

The change in sensor system height is represented by  $\Delta h$ , due to the  $i$ -<sup>th</sup> sensor reading change,  $\Delta d_i$  when  $\alpha$  remains constant.

$$\Delta h = \Delta d_1 \cos \alpha, \quad (10)$$

$$\Delta h = \Delta d_2 \cos(\alpha + \alpha_{12}), \quad (11)$$

$$\Delta h = \Delta d_3 \cos(\alpha + \alpha_{12} + \alpha_{23}). \quad (12)$$

If the floor is even, then the height change due to three sensor readings should be the same;

$$\begin{aligned} \Delta d_1 \cos \alpha &= \Delta d_2 \cos(\alpha + \alpha_{12}) \\ &= \Delta d_3 \cos(\alpha + \alpha_{12} + \alpha_{23}). \end{aligned} \quad (13)$$

The change of the angle is represented by  $\Delta \alpha$  due to the  $i$ -<sup>th</sup> sensor reading change,  $\Delta d_i$  when  $h$  remains constant.

$$\Delta \alpha = \arccos\left(\frac{h}{d_1 + \Delta d_1}\right) - \arccos\left(\frac{h}{d_1}\right) \quad (14)$$

$$\Delta \alpha = \arccos\left(\frac{h}{d_2 + \Delta d_2}\right) - \arccos\left(\frac{h}{d_2}\right) \quad (15)$$

$$\Delta \alpha = \arccos\left(\frac{h}{d_3 + \Delta d_3}\right) - \arccos\left(\frac{h}{d_3}\right) \quad (16)$$

If the floor is even, then the change of the angle due to three sensor readings should be the same; (14), (15) and (16) provide another condition for identifying an even floor. From these conditions, one must determine whether the floor is even or not. In case it is not, then a new floor model is made from the sensor readings by calculating the end point position of each sensor ray and the environment model is updated. This function is called a 'Floor state estimator' in this paper

It is reasonable to use the probabilistic model of the system because there exist uncertainties in localization and measurements. For simplicity, a 2D model (Fig. 5) is used for explanation of the analysis. The point D represents the location of the floor where the range sensor ray hits. Three sensors are used in the sensor system, and the analysis with the first sensor (S1 in Fig. 4) is described first. The base (A) may have uncertainties in position and orientation. Because the supporting foot touches the ground, the uncertainty in the Y-direction is regarded as the uncertainty of the surface height and the uncertainty in orientation is due to surface slope. The previous section mentioned the assumption that the position control error of each joint is negligible, meaning zero error covariance. Therefore the uncertainties of point B is calculated using a homogenous transformation, which represents the forward kinematics from A to B, and the covariance analysis.

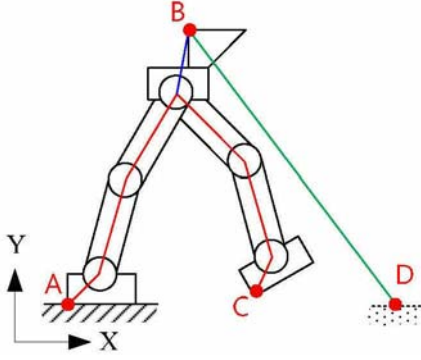


Fig. 5. Simplified 2D model.

Representing the uncertainties of the base (A) using the error covariance matrix  $C_A$ ,

$$C_A = \begin{bmatrix} \sigma_{A,x} & 0 & 0 \\ 0 & \sigma_{A,y} & 0 \\ 0 & 0 & \sigma_{A,\theta} \end{bmatrix} \quad (17)$$

and the uncertainties of the sensor system origin (B) using  $C_B$

$$C_B = \begin{bmatrix} \sigma_{B,x} & 0 & 0 \\ 0 & \sigma_{B,y} & 0 \\ 0 & 0 & \sigma_{B,\theta} \end{bmatrix}. \quad (18)$$

The uncertainties of the position and orientation of the sensor system origin (B) is represented using the propagated uncertainties,

$$C_B = F_A C_A F_A^T, \quad (19)$$

where  $F_A$  is the Jacobian matrix defined as

$$F_A = \begin{bmatrix} \frac{\partial X_B}{\partial X_A} & \frac{\partial X_B}{\partial Y_A} & \frac{\partial X_B}{\partial \theta_A} \\ \frac{\partial Y_B}{\partial X_A} & \frac{\partial Y_B}{\partial Y_A} & \frac{\partial Y_B}{\partial \theta_A} \\ \frac{\partial \theta_B}{\partial X_A} & \frac{\partial \theta_B}{\partial Y_A} & \frac{\partial \theta_B}{\partial \theta_A} \end{bmatrix}, \quad (20)$$

where  $[X_B \ Y_B \ \theta_B \ 0]^T$  are represented using the homogeneous transformation matrix multiplied by  $[X_A \ Y_A \ \theta_A \ 0]^T$ .

The uncertainties of the position of the other foot end (C) are represented similarly. In order to include the uncertainties of the sensor readings, the error covariance matrix of  $B$  is redefined as

$$C_B^* = \begin{bmatrix} \sigma_{B,x} & 0 & 0 & 0 \\ 0 & \sigma_{B,y} & 0 & 0 \\ 0 & 0 & \sigma_{B,\theta} & 0 \\ 0 & 0 & 0 & \sigma_d \end{bmatrix}, \quad (21)$$

so that the uncertainties of the sensor values are augmented. Those values are measured from experiments with

respect to their range. The uncertainties of the point  $D$ ,

$$C_D = \begin{bmatrix} \sigma_{D,x} & 0 \\ 0 & \sigma_{D,y} \end{bmatrix} \quad (22)$$

are calculated from

$$C_D = F_B C_B^* F_B^T, \quad (23)$$

where

$$F_B = \begin{bmatrix} 1 & 0 & d \cos(\theta_B + \alpha) & \sin(\theta_B + \alpha) \\ 0 & 1 & d \sin(\theta_B + \alpha) & -\cos(\theta_B + \alpha) \end{bmatrix}. \quad (24)$$

The analysis with the second sensor (S2 in Fig. 4) is the same as above, except that (24) becomes

$$F_B = \begin{bmatrix} 1 & 0 & d \cos(\theta_B + \alpha + \alpha_{12}) & \sin(\theta_B + \alpha + \alpha_{12}) \\ 0 & 1 & d \sin(\theta_B + \alpha + \alpha_{12}) & -\cos(\theta_B + \alpha + \alpha_{12}) \end{bmatrix}. \quad (25)$$

Similarly, for the analysis with the third sensor (S3 in Fig. 4), equation (24) becomes

$$F_B = \begin{bmatrix} 1 & 0 & d \cos(\theta_B + \alpha + \alpha_{12} + \alpha_{23}) & \sin(\theta_B + \alpha + \alpha_{12} + \alpha_{23}) \\ 0 & 1 & d \sin(\theta_B + \alpha + \alpha_{12} + \alpha_{23}) & -\cos(\theta_B + \alpha + \alpha_{12} + \alpha_{23}) \end{bmatrix}. \quad (26)$$

Please note that  $d$  in (24), (25) and (26) represents the sensor reading of the corresponding range sensor.

Other important sensors used are the gyros (ADIS16100 from Analog Digital) for roll, pitch and yaw angular velocity measurements, and the accelerometers (LIS3LV02DQ from ST) for 3-axis acceleration measurements. Those are installed on top of the infrared range sensor systems as shown in Fig. 6. The sampling rates for the gyros and accelerometers are 100 Hz. Even though it's obvious that integrating the acceleration twice provides the displacement, and integrating the angular velocity yields angular displacement, those sensors have drift errors and the localization accuracy is very vulnerable to these errors. As such, these sensors are used for contact



Fig. 6. Humanoid robot with sensors.

estimation rather than localization information. This paper calls this function a ‘contact estimator’. Whenever a foot hits the floor, a large impact occurs and the magnitude of the acceleration peaks. Therefore, one can tell whether the robot walks as planned in the modeled environment by monitoring the acceleration peak. The yaw/pitch/roll gyro outputs indicate any momentary loss of balance. The sensor threshold values for differentiating these events are set from experiments. If the instant when large peak occurs is not the same as expected, then it tells the motion planner that the floor model is not correct and also lets the robot forward kinematics update the landed foot height.

The controller embedded in the robot controls the servo motors. It also feeds each joint angle and sensor readings back to the main controller, which is a notebook computer for high computing power. The main controller is composed of several functional modules. Fig. 7 shows the controller architecture.

If the following assumptions are met, then the contact estimator is not necessary.

- floor environment is completely known or modeled without error from measurements
- localization error is zero

The motion planner is composed of two parts; global path planner and step planner. For a given environment, the global planner generates a collision free path. This paper only considers 2-D planar environments and all the obstacles are assumed to be too high to be stepped over. The step planner then divides the path into many segments such as normal step, half-step, normal-side step, halfside-step for humanoid robot walking. For each segment, the angle commands are generated for all joints. Change of robot orientation is also implemented with a slight turning step or rotation of the body depending on the radius of the path curvature. [Single support - Double support] and [Deploy - Swing - Heel contact] phase makes one complete walking cycle. Even though the floor is assumed to be even initially, if the floor is sensed to be non-flat and the estimated height or depth of the irregular surface is within the preset value (30 mm for

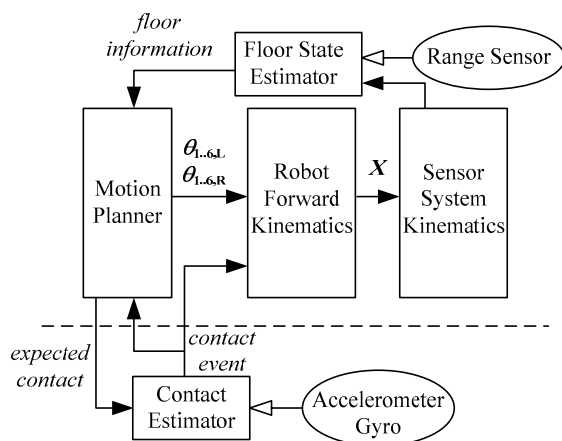


Fig. 7. Controller architecture.

experiments in this paper), then the step planner generates a step-on or step-off motion. The floor information is registered to update the environment model.

The three infrared range sensors, gyro and accelerometer readings are sampled every 10 msec. The desired joint angles are generated a priori from the motion planner and stored in the servo controller memory. Those are provided to each servo motor every 10 msec. The pre-generated joint commands are also used to calculate the position and orientation of the sensor system in the sensor system kinematics module in Fig. 7. With the results of the range sensor readings and sensor system kinematics, the floor state is estimated using (4)-(16) every 10 msec in the main controller (notebook computer).

#### 4. EXPERIMENT

The following figure shows the floor model with three range sensor measurements. Sensor 3 (S3 in Fig. 2) is the one which has the largest incident angle to the floor and has the longest range readings, thus it has the largest variations. In Fig. 8, the floor is slanted 0.5 m away from the origin. The estimated surface from the three sensor readings follows the real surface with small variations. The estimated floor state information is used to update the environment (floor) model.

The assumptions are not realistic most of the time. In case one of the robot’s feet hits the floor higher than expected, the base of the kinematics changes, thus the estimated position and orientation of the robot becomes incorrect. Therefore, it is very important to constantly monitor if the robot’s moving foot hits the floor as expected. If it hits the floor earlier than planned, it is most likely that the floor is higher than modeled. In such cases, the accelerometer reading changes abruptly earlier than the foot is expected to hit the floor. If the floor is lower than modeled, then the robot’s pitch and/or roll, yaw angles may abruptly change right after the foot is expected to hit the floor. In such cases, the gyro and accelerometer readings indicate such events very effectively. Figs. 9 and 10 show the robot is walking without knowing that the floor is elevated 35 cm away from the origin.

It usually happens that the robot yaw angle changes significantly when one foot hits the floor earlier than expected as shown in Fig. 10.

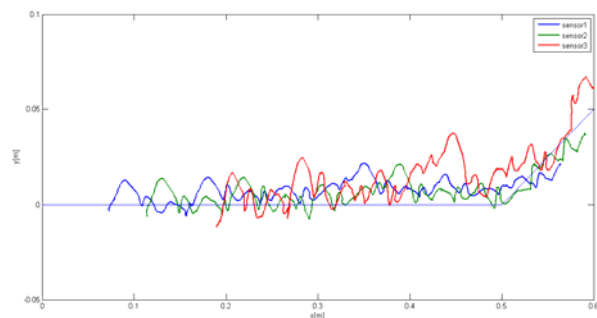


Fig. 8. Estimation of Slope.

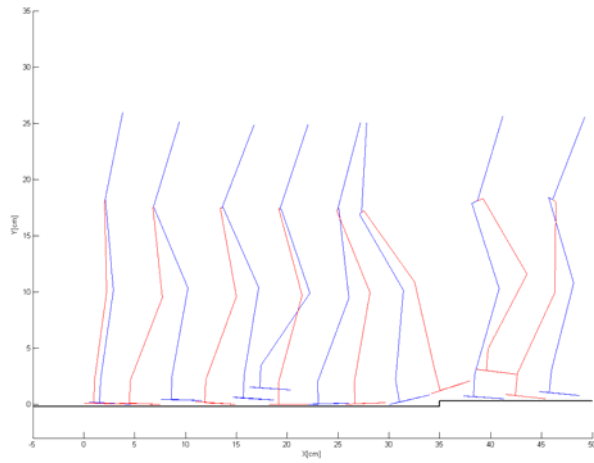


Fig. 9. Walking without floor estimation.

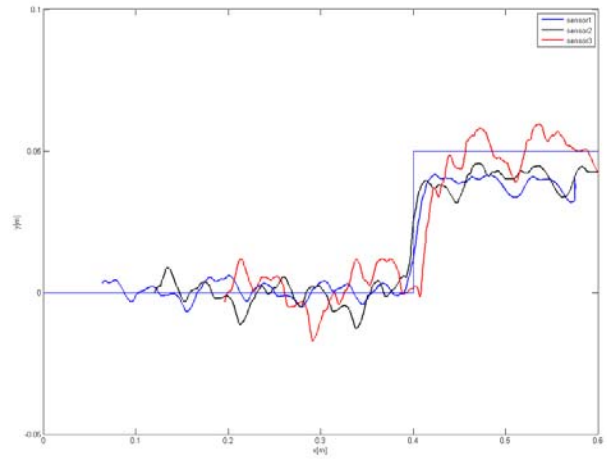


Fig. 12. Estimation of a Step.

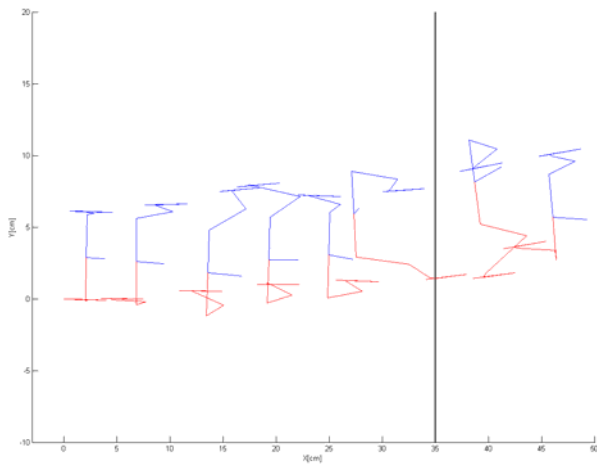


Fig. 10. Walking without floor estimation (Top view).

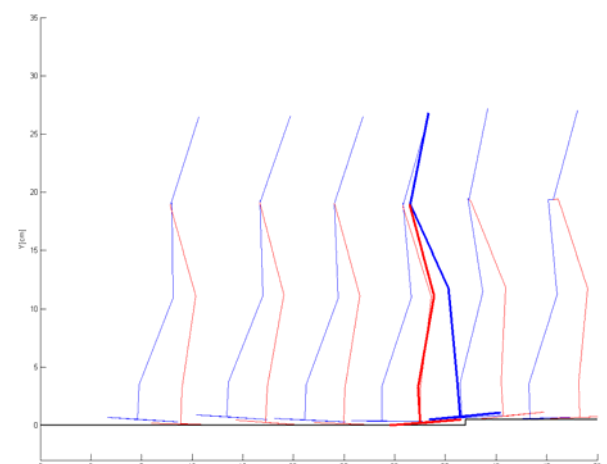


Fig. 13. Walking with floor estimation.

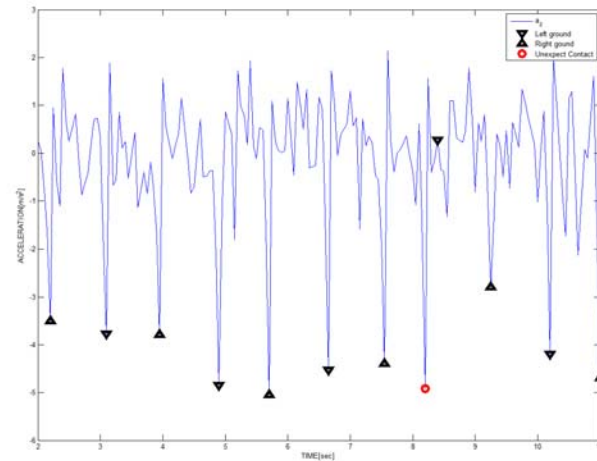


Fig. 11. Accelerometer readings.

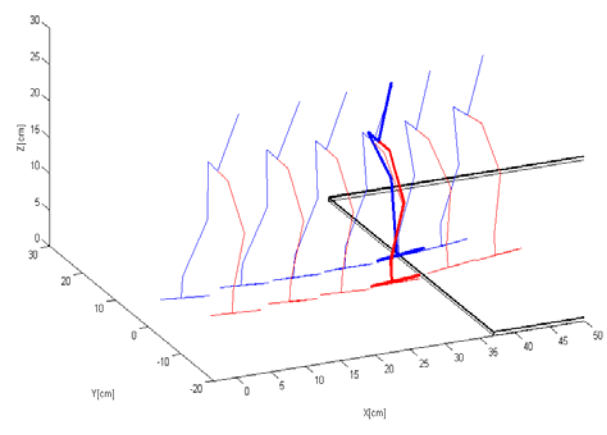


Fig. 14. Walking with floor estimation (3D).

The following figure shows the accelerometer outputs. The magnitude of the acceleration in the Z-direction becomes large when the left or right foot hits the floor. The triangles show these incidents. If the time of the incident is not the same as expected by the motion planner, then the floor is not the same as the environment model. The circles in the figure indicates the impact occurred earlier than expected (upside down triangle

between 8 and 9 seconds) because the floor is higher than the model.

With the range sensor system, the result of the floor elevated 0.4 m away from the origin is identified as shown in Fig. 12.

With this environment model, the motion planner generates paths accordingly, and the robot walks on the floor successfully as shown in Figs. 13 and 14.

## 5. CONCLUSION

In order to perceive the floor state and to model the environment for walking, a range sensor system is developed. Measurement from the sensors built in the humanoid robot requires correct kinematics. The accelerometer and the gyro sensors are used to detect the interaction between the foot and the surface. The main controller, composed of a motion planner, kinematics, and a contact estimator, use all the sensor information for localization and safe walking. The uncertainties are considered with covariance analysis. The experimental results show the effectiveness of the proposed sensor information analysis.

## REFERENCES

- [1] C. Fu and K. Chen, "Gait synthesis and sensory control of stair climbing for a humanoid robot," *IEEE Trans. on Industrial Electronics*, vol. 55, no. 5, pp. 2111-2120, 2008.
- [2] J. Y. Kim, I. W. Park, and J. H. Oh, "Walking control algorithm of biped humanoid robot on uneven and inclined floor," *Journal of Intelligent and Robotic Systems*, vol. 48, no. 4, pp. 457-484, 2007.
- [3] C.-S. Park, T. Ha, J. Kim, and C.-H. Choi, "Trajectory generation and control for a biped robot walking upstairs," *Int. Journal of Control, Automation and Systems*, vol. 8, no. 2, pp. 339-351, 2010.
- [4] K. Okada, T. Ogura, A. Haneda, and M. Inaba, "Autonomous 3d walking system for a humanoid robot based on visual step recognition and 3D foot step planner," *Proc. of the IEEE International Conference on Robotics and Automation*, pp. 623-628, 2005.
- [5] J. Gutmann, M. Fukuchi, and M. Fujita, "3D perception and environment map generation for humanoid robot navigation," *Int. Journal of Robotics Research*, vol. 27, no. 10, pp. 1117-1134, 2008.
- [6] M. Heracles, B. Bolder, and C. Goerick, "Fast detection of arbitrary planar surfaces from unreliable 3D data," *Proc. of IEEE/RSJ Int. Conference on Intelligent Robots and Systems*, pp. 5717-5724, 2009.
- [7] S. P. N. Singh and K. J. Waldron, "Attitude estimation for dynamic legged locomotion using range and inertial sensors," *Proc. of the Int. Conference on Robotics and Automation*, pp. 1663-1668, 2005.
- [8] M. Gienger, K. Löffler, and F. Pfeiffer, "Walking control of a biped robot based on inertial measurement," *Proc. of the Third IARP Int. Workshop on Humanoid and Human Friendly Robotics*, pp. 22-29, 2002.
- [9] H. Rehbinder and X. Hu, "Drift-free attitude estimation for accelerated rigid bodies," *Proc. of the IEEE International Conference on Robotics and Automation*, pp. 4244-4249, 2001.
- [10] R. Henrik and H. Xiaoming, "Nonlinear pitch and roll estimation for walking robots," *Proc. of the IEEE Int. Conf. on Robotics and Automation*, pp. 2617-2622, 2000.
- [11] M. Lee and S. Lee, "Design and analysis of an

infrared range sensor system for floor-state estimation," *Journal of Mechanical Science and Technology*, vol. 25, no. 4, pp. 1043-1050, 2011.



**Sooyong Lee** received his B.S. and M.S. degrees in Mechanical Engineering from Seoul National University, Seoul, Korea, in 1989 and 1991, respectively, and his Ph.D. degree from MIT, Cambridge, MA, in 1996. He worked as a Senior Research Scientist at KIST and then as an Assistant Professor in the Department of Mechanical Engineering at Texas A&M University. He joined Hongik University, Seoul, Korea in 2003 and is currently a Professor in the Mechanical and System Design Engineering Department. His current research includes mobile robot localization and navigation, and active sensing.



**Paul Y. Oh** received mechanical engineering degrees from McGill (B.Eng 1989), Seoul National (M.Sc 1992), and Columbia (Ph.D. 1999) universities. Paul Oh is a full professor and ASME Fellow at Drexel University's Mechanical Engineering Department. From 2008-2010, he served at the National Science Foundation (NSF) as the Program Director managing the robotics research portfolio. He has authored over 90 referred archival papers and edited 2 books in the areas of robotics and unmanned systems. Honors include faculty fellowships at NASA Jet Propulsion Lab (2002), Naval Research Lab (2003 and 2013), the NSF CAREER award (2004), the SAE Ralph Teetor Award for Engineering Education Excellence (2005) and being named a Boeing Welliver Fellow (2006). He is the Director of the Drexel Autonomous Systems Lab and also the Founding Chair of the IEEE Technical Committee on Aerial Robotics and UAVs.